

Scalable Quantum Dot Amplifier Based Optical Switch Matrix

A. Albores-Mejia, K.A. Williams, T. de Vries, E. Smalbrugge, Y.S. Oei, M.K. Smit, S. Anantathanasarn, R. Nötzel

TU Eindhoven, Eindhoven, The Netherlands

a.a.m.albores.mejia@tue.nl

Abstract. *A quantum dot active layer is used in a novel, highly scaleable monolithic optical switch matrix architecture. Electronically paired semiconductor optical amplifiers gates are implemented in a four-input four-output configuration to reduce the electrical connections and control complexity. Low power penalty 10Gb/s routing at a wavelength of 155nm is demonstrated.*

Increasingly high-capacity data transfer in storage area networking, high performance computing, and server networks is driving research into increasingly elaborate photonic switched interconnect test-beds [1-4]. The need for low-latency, high capacity, scalable switch fabrics with low driver complexity, excellent crosstalk and the broad gain bandwidth has lead to a particular focus on semiconductor optical amplifier (SOA) based switches. However, considerable integration is required to remove complex packaging-related restrictions such as the high numbers of fibre pigtailed, power consuming cooler circuits, and the complex electronic control circuits.

To date, integrated SOA based switch designs have focused on gate arrays in a broadcast and select architecture. The gates and inputs are connected via splitters and combiners utilising fibre [4] and waveguides with hybrid integration [5] and epitaxial regrowth [6]. The latter has lead to the smallest circuits with 20mm² footprints. The bulk active layer amplifier designs implemented have however lead to low saturation powers. The resulting low distortion threshold necessitates a lower number of photons per bit and thereby impairs signal to noise ratio and data capacity. The broadcast and select architecture requires a high number of waveguide crossings and exhibits a square law scaling in the required electrical control signals with the number of optical inputs. This already leads to 16 independent controls for a four input four output switch.

In this work, we present the first implementation of a four input, four output quantum dot based switch matrix. The design is based on a new crossbar element design which both integrates the waveguide crossing within the gate and is implemented with common electrodes to halve the required numbers of electrical connections. The use of complementary electrical signals further halves the number of independent control signals to four. Integration of the crossing within the gate also allows a reduced size for the shuffle network, and in combination with low loss, low distortion, quantum dot epitaxy, this allows an all-active implementation in a reduced chip area of only 3mm².

Integration Architecture

Figure 1i shows a photograph of the fabricated circuit. Four parallel input and output waveguides on a 250µm pitch are shown on the left and right hand side of the image. At the centre, a reduced shuffle network is implemented to interconnect the four crossbar switches. This therefore allows any optical input to be pathed to any optical

output by means of electronic addressing, although not necessarily simultaneously. Non-blocking operation may be implemented with a third stage of crossbars, but contention may also be more efficiently addressed with a packet-time-scale media access protocol.

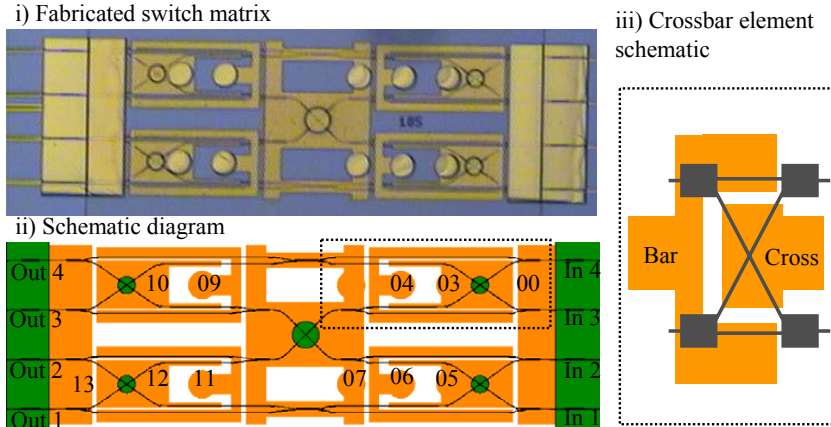


Figure 1: i) Photograph of switch matrix prior to bonding.
 ii) Schematic layout showing waveguides and metallisation in correct proportion.
 iii) Logical representation for one crossbar element.

The paths are implemented with a combination of multimode interference splitters and combiners located within the input, shuffle and output regions (pads 00, 07 and 13 in figure 1ii). These are interconnected by two stages of cascaded SOA gates (pads 03-06 and 09-12) which are also electronically configured. A crossing is implemented within the gates themselves using tight bend radius $100\mu\text{m}$ curves in combination with shallow-etched orthogonal crossings. This allows the area required for the remaining crossings and connections to be significantly reduced. The metallisation is common between the paths for the input, output and central shuffle region (pads 00, 07, 13). Within the crossbar matrix element, pairs of gates are electronically coupled to each other to reduce the off-chip wiring. One such crossbar matrix element is highlighted by the dashed box in figure 1ii with its logical equivalent alongside. For the two logical operational states required: cross and bar, this leads to a requirement for only one control input per crossbar switch, further reducing the operational complexity. Only four independent control signals are required for the four input, four output matrix.

The switch matrix is fabricated from a five stack quantum dot active plane embedded in a $Q1.15\mu\text{m}$ InGaAsP separate confinement heterostructure [7]. A single step all-active epitaxy is used. The lower schematic in Figure 1ii shows the connections for the switch matrix. Three of the mask layers are shown including the SOA waveguide layer in black, p-metallisation denoted by the light shading, and regions with shallow SOA waveguides denoted by the dark shading. While the mask layer for the electrical isolation is not shown, the InGaAs capping layer is removed between the metal areas for this purpose. Planarisation is performed prior to gold evaporation and plating. Devices are mounted as-cleaved, epoxy bonded to patterned ceramic tiles, and wire bonded.

Circuit element performance

The switch is assessed using a multi-probe to the ceramic tile in combination with a reconfigurable electronic multiplexer. Forward series resistance values between 4-6 Ω are measured depending on the addressed waveguides with one electrical fail at pad 5. Electrical isolation is measured to be in excess of 100k Ω for all electrode combinations. Initial characterisation is performed without electrical bias as the quantum dot epitaxy is sufficiently low loss to enable such characterisation and this is expected to provide clearer insight into on-chip component performance. Photocurrent measurements were performed for each circuit element with a continuous wave optical input of -13.7dBm in-fibre. Figure 2 shows the photocurrent generated at each electrical connection with the remaining connections left open circuit. Both forward and reverse directions through the circuit are overlaid with separate axes to show responses to all eight optical inputs. The data indicate a relatively uniform optical performance throughout the circuit. Predicted photocurrent values are also shown for the circuit with a solid line in figure 2 assuming the designed de/multiplexing gain and 4dB combiner losses.

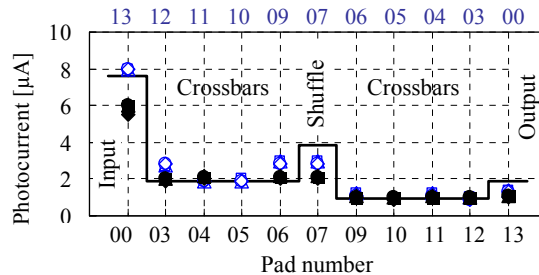


Figure 2: Measured photocurrent for -13.7dBm in-fibre injected power for each input (open symbols) and output (filled symbols). The solid line shows the predicted values.

A mean photocurrent reduction of 9dB is observed from the input pin to the output pin. The mean fibre coupling loss is estimated to be 8dB per facet from photocurrent measurements and this includes an estimated loss of 1.5dB through the cleaved facet. Including a 6dB adjustment to account for the four optical outputs gives a predicted fibre to fibre loss of 31dB for the unbiased circuit. This may be compared with direct power measurements at the input and output fibres where best case fibre coupled measurements give a 36dB off-state loss. More typical values of around 40dB are also measured for the majority of paths. A discrepancy is expected from difficulties in precisely estimating fibre coupling loss and from output waveguide losses which are unaccounted for in the photocurrent measurements.

Continuous wave currents are subsequently applied to combinations of five electrodes to form the switch paths. The input, output and shuffle pins are each operated at 200mA. The crossbar electrodes are selected according to the required state and are biased at 100mA. When one crossbar element is switched from on to off state, crosstalk values of over 10dB are typically observed. Local heating is believed to compromise the available gain and therefore crosstalk. Improved confinement layer design and longer gate length in the crossbar elements is expected to directly enhance performance. Optical saturation properties have also been studied, with the dependence of the gain on input fibre coupled power being negligible up to +11dBm.

10Gb/s Routing

To assess the integrity of routed data, optical eye diagrams and bit error rate measurements were performed at a data rate of 10Gb/s with a pattern length of $2^{31}-1$. A fibre-coupled input power of +11dBm is used to study stressed performance. The switch matrix is polarisation sensitive and the injected state is optimised for minimum path loss. The bias conditions are the same as for the previous crosstalk assessment. Measurements are shown for the path from input 3 to output 4 to give a 0.4dB power penalty. Eye diagrams before and after the matrix remain clearly open.

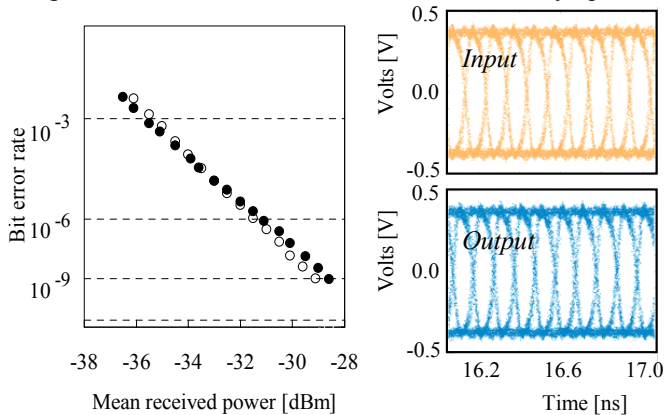


Figure 3: Bit error rate at 10Gb/s as a function of received power with (solid symbols) and without (open symbols) the switch matrix and corresponding eye diagrams.

Conclusions

The first quantum dot SOA based crossbar switch matrix design is proposed, fabricated and demonstrated. The monolithic circuit exploits the low loss and low distortion properties of the epitaxy to enable a compact, all-active, four input, four output switch fabric. The architecture leads to a marked reduction in electrical connections and control complexity compared to previously published SOA based switch arrays. A low optical power penalty of only 0.4dB is observed when routing 10Gb/s data.

References

- [1] A. Shacham, B. A. Small, O. Liboiron-Ladouceur, and K. Bergman, *J. Lightwave Technol.* 23, 3066–3075 (2005).
- [2] R. Luijten, C. Minkenberg, R. Hemenway, M. Sauer, and R. Grzybowski, *Proceedings of the 2005 ACM/IEEE Conference on Supercomputing*, p. 18.
- [3] T. Lin, K. A. Williams, R. V. Penty, I. H. White, M. Glick, *J. Lightwave Technology*, 25 (3): 655–663 2007
- [4] G. Soulage, A. Jourdan, P. Doussiere, M. Bachman, J. Y. Emery, J. Da Loura, and M. Sotom, *European Conference on Optical Communication (1996)*, vol. 4, p. 145, paper ThD.2.1.
- [5] J. Sasaki, H. Hatakeyama, T. Tamanuki, S. Kitamura, M. Yamaguchi, N. Kitamura, T. Shimoda, M. Kitamura, T. Kato, and M. Itoh, *Electron. Lett.* 34, 986–987 (1998).
- [6] W. van Berlo, M. Janson, L. Lundgren, A.C. Moerner, J. Terlecki, M. Gustavsson, P. Granstrand and P. Svensson, *IEEE Photonics Technology Letters*, 7, 11, 1291–1293, 1995
- [7] R. Nötzel, S. Anantathanasarn, P.J. van Veldhoven, F.W.M. van Otten, T.J. Eijkemans, A. Trampert, B. Satpati, Y. Barbarin, E.A.J.M. Bente, Y.S. Oei, T. de Vries, E.J. Geluk, E. Smalbrugge, M.K. Smit, and J.H. Wolter, (Review Paper), *Jpn. J. Appl. Phys.* 45, 6544–6549 (2006).